Pergamon

Int. J. Solids Structures Vol. 32, No. 2, pp. 173–201, 1995

0020–7683/95 $9.50 + .00

0020–7683(94)00133–2

SYMMETRY AND OTHER GEOMETRIC CONSTRAINTS OF SURFACE NETWORKS IN NATURE AND SCIENCE

Z. YONG
Department of Engineering Mechanics, University of Kentucky, Lexington, KY 40506-0046, U.S.A.

(*Received* 26 *February* 1994; *in revised form* 6 *June* 1994)

Abstract—Three basic equations for topological constraints upon inhomogeneous surface networks of solids are derived from the Euler equation and other identities which lead to some insight into the essential issues of this area. In particular, a symmetry between vertices and polygons of a general surface network is shown to exist, and variations in a surface network can simply be described as a kind of reciprocal exchange between vertices and polygons. The number of three-ordered or three-fold vertices, as well as many-edged polygons and many-ordered vertices, is controlled by the ratio of the number of three-edged and/or four-edged polygons to the total number of polygons. When the minimum-edged polygon has five edges, the number of three-ordered vertices is automatically greater than two-thirds of the total number of vertices. The dominant occupation of three-ordered vertices can still retain under certain conditions after appearance of three-edged and/or four-edged polygons. The critical distribution of polygons for the maintenance of this kind of domination is determined. The gap between the critical distribution and natural or artificial surface networks allows the geometric structure of a network to be changed greatly without loss of the domination. This finding establishes a quantitative basis for the description of granular and biological materials in terms of microstructures. It will also be seen that classical models correspond to a very special case of constraints. Theoretical results are in agreement with experimental data for networks that arise in surfaces, such as fracture, biological cells, metallurgical grains, bubbles, leaf-vein networks and the coat pattern of a giraffe.

1. INTRODUCTION

Surface networks are very prevalent geometric structures in nature, ranging in scale from the microscopic to the macroscopic. In general, they fall into two categories: skeletal and non-skeletal surface networks. The commonest skeletal network is the trajectory of a moving object, such as a spider's web, whereas a non-skeletal network usually consists of boundaries of condensed matter, such as leaf-vein networks of trees, as shown in Fig. 1. The attention of the present work focuses on non-skeletal networks. For brevity, therefore, a surface network is here assumed to be non-skeletal unless a skeletal network is specified. Nevertheless, the results obtained are valid for both kinds of networks.

A surface network may exhibit a random form that stems from its own specific situation. Such forms may greatly deviate from each other in their function and role, as exemplified by the difference between the coat pattern of a giraffe and the crack network of soil, as shown in Figs 2 and 3. Mathematically speaking, however, any surface network can be simply described as arrangements of the basic geometric elements, points and edges, in the form of polygons. To gain insights into the underlying mechanisms of evolution and formation of a surface network, therefore, it makes sense to apply the mathematical principles of geometry to determine potential restrictions that might be imposed on the structures. Usually, these restrictions are referred to as space-filling requirements. One may note that conventional methods are no longer sufficient to overcome the difficulties that are rooted in the structure analysis of a general network. This difficulty arises because edges of polygons forming the network do not have to be straight or smooth lines with definite orientations but can be either plane or spatial irregular curves scatted randomly. In such circumstances, the principles of topology are indispensable.

Experimental observations and theoretical discussions on a wide variety of networks conducted by Thompson in 1917 were possibly one of the earliest works using topological

concepts in the field of structural analysis (see Thompson, 1963). During the past 80 years, many researchers made efforts to apply topological concepts, particularly the Euler equation, to quantify geometric requirements on the evolution and formation of a surface network. A brief review on such research activities prior to 1952 was given by Smith (1952). Motivated by identification of geometric constraints on metallurgical grain arrays, the research carried out by Smith (1952) systematically elaborated on the illustration of basic topological concepts, the description of constraint rules and the formulation of a quantitative procedure. Late developments, which were directed mainly towards applications of previously-established theories, were reviewed by Dormor (1980) for biological cellular networks, Weaire and Rivier (1984) for universal networks and Atkinson (1988) for metallurgical grain networks, respectively. Recent progress was also summarized by Anderson and Rollett (1990) in connection with the computer simulation of metallurgical grain growth. The topological requirements upon the formation of a surface network seem to be also significant in some other emerging areas of research, such as in the modeling of failure of thin films (Meakin, 1988, 1991) and in the simulation of coat patterns of animals (Murry, 1989; Sleeper, 1993).

Some topological constraints on the fragmentation of solid materials were investigated both theoretically and experimentally by Yong *et al.* (1994). Additionally, the analysis of topological constraints on the stress trajectory has unveiled certain difficulties in the local equilibrium theory of solid mechanics (Yong, 1994a). An example is also given in the latter part of Section 4 of this paper to illustrate the application of topological constraints to deriving the governing equation for fragmentation parameters. The present research is a continuation of the previous work and it is motivated by the following issues.

(1) One of the most important geometric phenomena, the formation of three-ordered or three-fold vertices, has long been assumed as the direct consequence of physical effects (e.g. Smith, 1952; Dormor, 1980; Glazier *et al.* 1990). From the geometric point of view, a typical shortcoming of this assumption is the isolation of vertex order from the distribution ratios of different polygons. Sometimes the three-ordered vertices are ascribed to topological stable structures, or it is assumed that the topological properties are unchanged by small deformations (Weaire and Rivier, 1984; Atkinson, 1988). However, a topological property should not be related to small deformations, since it is independent of the size and shape of a geometric object. Even though physical mechanisms behind the growth of a network might be consistent, more or less, with certain geometric phenomena, the current theories seem to restrict a universal topological property within a limited domain.

(2) Exclusion of the negative Euler characteristics in classical models has oversimplified the diversity of natural and artificial structures. The conventional representation of a flat network is based on the map of a sphere coordinated by a projective plane (see Blackett, 1967), and, therefore, its Euler characteristic is 2. This type of model is valid only for a simply connected plane. In this circumstance, any inhomogeneous defects which may appear during the evolution of a network or exist previously cannot be distinguished from normal cells. In other words, many previous models must indifferently treat all cells of a network, otherwise the Euler equation no longer holds at all. In association with surface networks, inhomogeneity is not rare, but is a very common phenomenon. For example, the manifest inhomogeneous defects caused by numerous large vessels were observed in the cellular networks of trees (Zimmermann and Brown, 1971, pp. 91–92). In this example, in sharp contrast with six, the average edge number of cells, the number of edges of a single vessel neighboring on cells is as high as 42. With regard to the physical effects of inhomogeneous defects, therefore, introduction of the negative Euler characteristics can be of practical value.

(3) To a certain degree, previous investigations of topological constraints seem to stay simply on the direct verification of the Euler equation. Few quantitative results exist for interactions between vertices and polygons. Consequently, a considerable number of challenging questions have no clear answers to date. For instance, what types of polygon play important roles in the formation of low-ordered vertices? Is there any specific relation between low-edged polygons and many-ordered vertices? Finally, the lack of a clearly understood mechanism for the distribution of many-edged polygons in a surface network

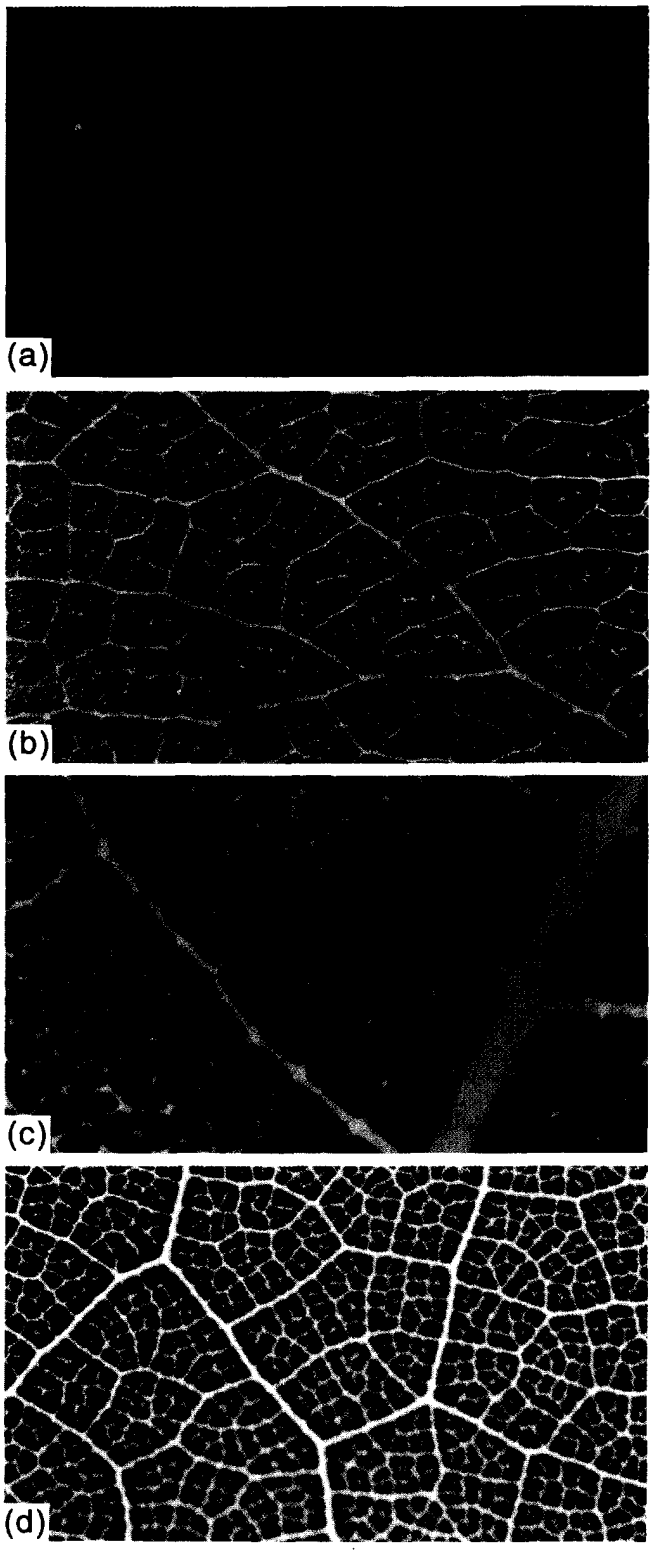

Fig. 1. Four leaf-vein networks.

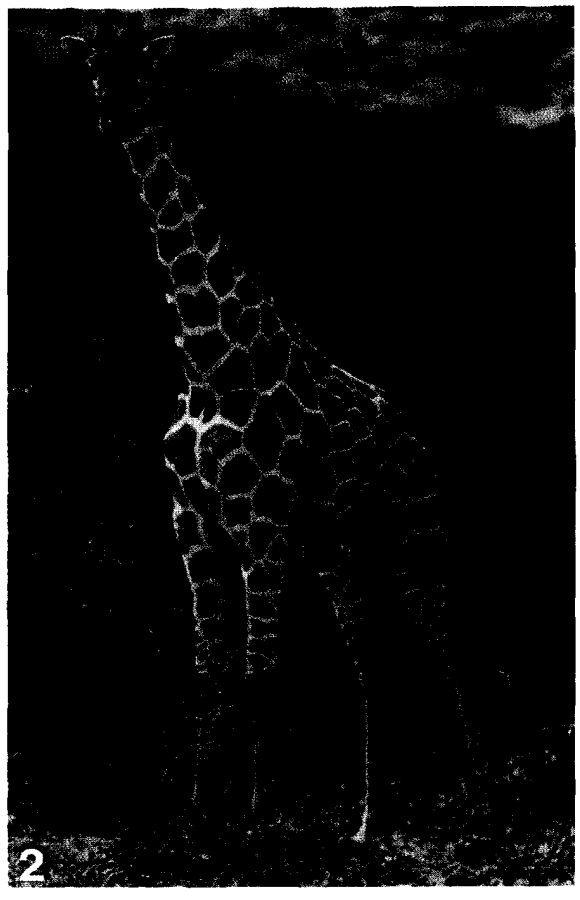

Fig. 2. The coat pattern of a reticulate giraffe from *The Giraffe* (Dagg and Foster, 1976), reproduced with the author's permission.

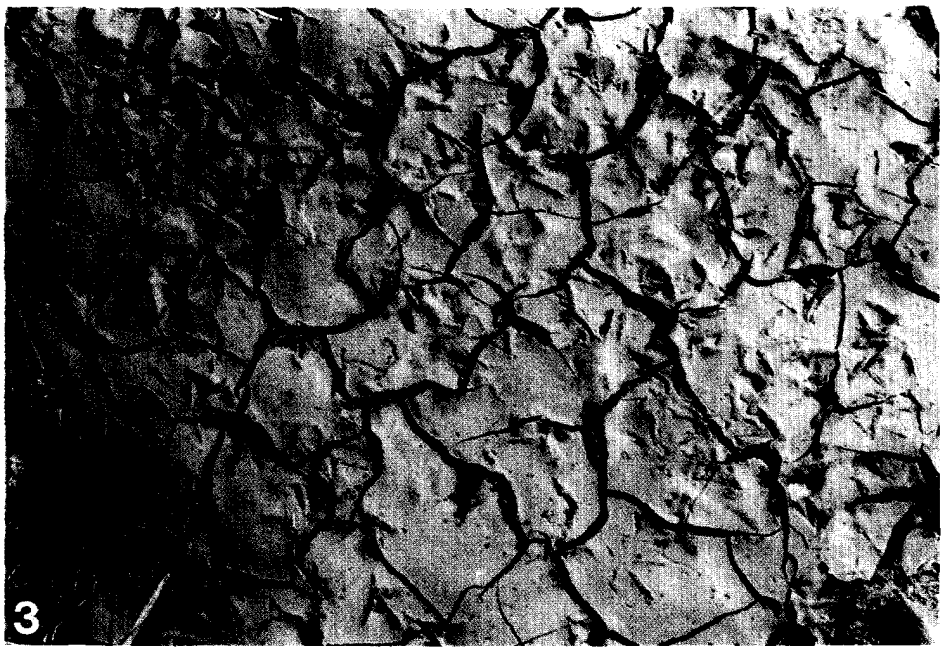

Fig. 3. A crack network on the soil ground.

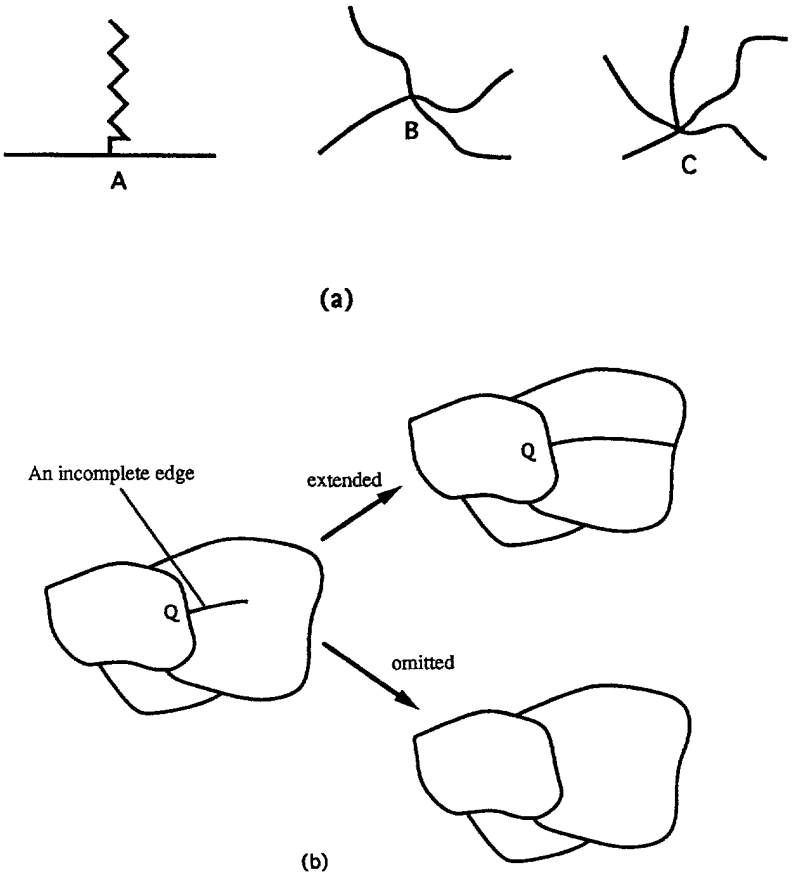

Fig. 4. (a) Three examples of vertices. (b) Illustration for the treatment of an incomplete edge.

has given rise to negative effects in modeling metallurgical grain growth (Glazier *et al.*, 1990). Therefore, new efforts are needed on other topological constraints of networks to meet the growing needs.

In order to obtain basic parameters which govern a surface network, the present research derives three new formulae from the Euler equation, as well as other usual identities. In addition, the plane representation of a many-holed torus is introduced to broaden the applicable scope of geometric constraints from homogeneous networks to inhomogeneous ones.

2. SOME BASIC CONCEPTS

Several topological terms have already entered this presentation, so at this point some definitions and concepts are here introduced to explain these terms and they will be used throughout the balance of the paper. For more details, the reader is invited to use the book by Blackett (1967). The first point to be used is that the topological property of a geometric object remains unchanged after subjected to a well-defined continuous transformation. Next, the following definitions are required.

Vertex and its order

A vertex is an intersection point of at least three curves (a straight line is the special case of a curve). It is marked by a letter. The order of a vertex is the number of the times that the vertex appears as the end of a curve. Vertices A–C shown in Fig. 4(a) are three-ordered, four-ordered and five-ordered vertices, respectively.

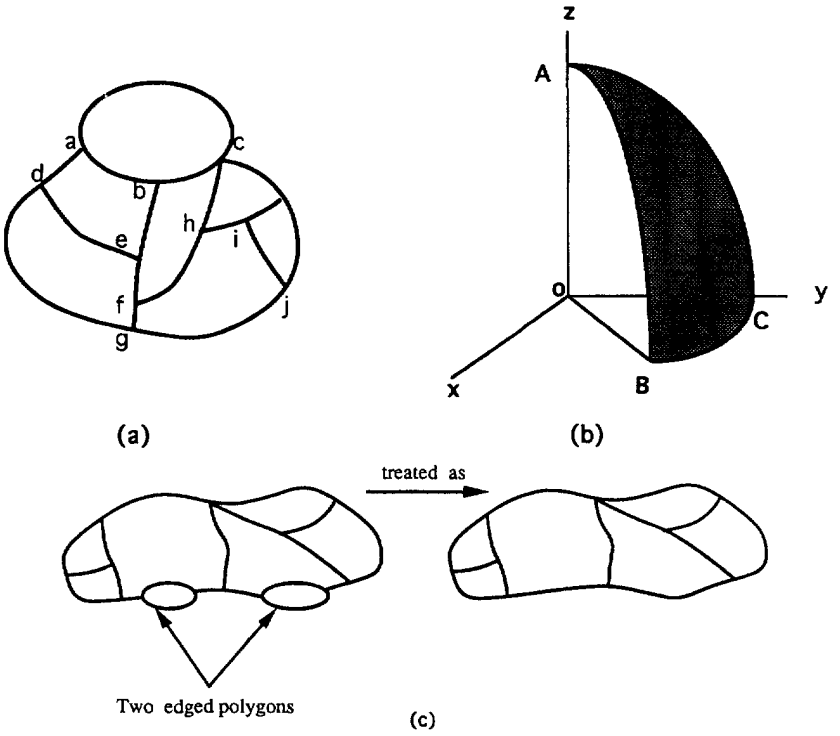

Fig. 5. (a) Examples of planar polygons. (b) Examples of spatial polygons. (c) Illustration for treatment of two-edged polygons.

Edge and polygon

An edge is a curve connecting two vertices. Sometimes, an incomplete edge may appear in a surface network as shown in Fig. 4(b). With no loss of generality, the incomplete edge will either be extended to intersect with another edge, or it will not be counted as an edge. In the latter case, intersection point Q will not be treated as a vertex. A polygon is a single closed ring consisting of at least three edges associated with three vertices. A polygon is denoted by marks of its vertices. In Fig. 5(a), planar polygon ⟨abc⟩ is a three-edged polygon, ⟨adeb⟩ and ⟨hijgf⟩ are four-edged and five-edged polygons, respectively. The non-planar polygon ⟨ABC⟩ shown in Fig. 5(b) is also a three-edged polygon. ⟨ABC⟩ is said to be topologically equivalent to ⟨AOC⟩, ⟨AOB⟩ or ⟨BOC⟩ or even ⟨abc⟩ of Fig. 5(a), because all of them have three edges. Very few two-edged polygons such as these shown in Fig. 5(c) are observed in surface networks. Of interest to us, they will be treated as an edge, moreover, in order to avoid derivations and discussions which do not serve the practical applications we have in mind.

Surface and surface network

A surface is the boundary of a finite object. A surface network is constructed by a group of polygons on a portion of the surface or on its entirety. Two surfaces or two surface networks will not be distinguished from each other unless the Euler characteristics of the two surfaces are different (the meaning of a Euler characteristic is explained below). For instance, two surface networks shown in Fig. 6(a,b) are considered to be equivalent because pattern (b) is generated from pattern (a) by using the mapping $z = |\cos(x^2+y^2)^{1/2}|$ under the Cartesian coordinates (x, y, z). Visibly, there is no difference about vertices and polygons between the two grid networks.

The Euler characteristic

The Euler characteristic, denoted by χ_E, is evaluated by the expression $\chi_E = 2-2N_E$ where N_E is a positive integer and it is called the number of holes of a *torus*. The Euler

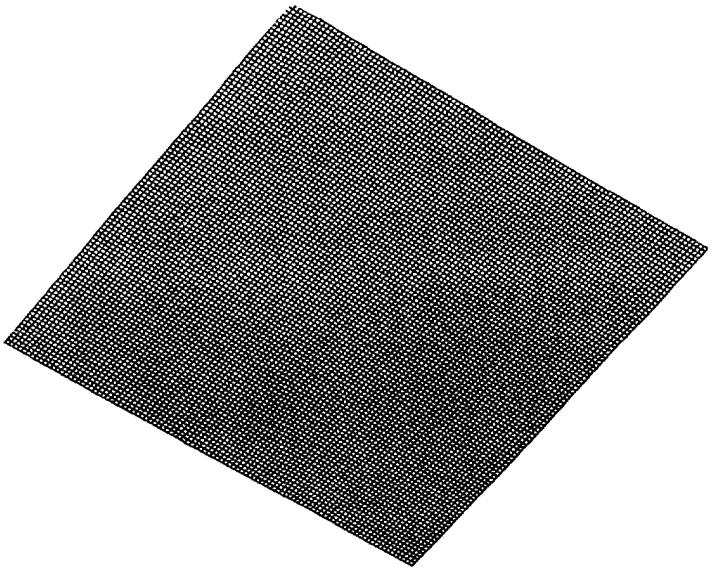

(a)

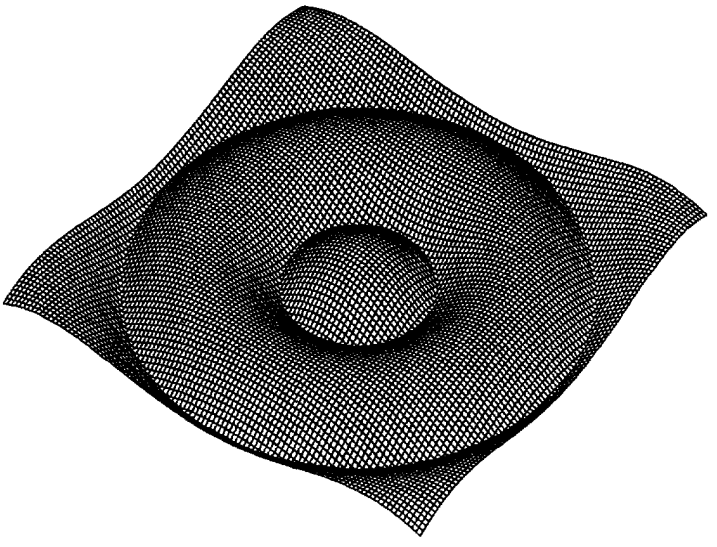

(b)

Fig. 6. Two equivalent surface networks. (a) A flat pattern. (b) A deformed pattern.

characteristic χ_E displays its significance when it is related to the subdivision of a torus into a polyhedron by the equation

$$N_0 - N_1 + N_2 = \chi_E, \tag{1}$$

where N_0 is the number of vertices on the torus, N_1 the number of edges and N_2 the number of polygons. The relation $\chi_E = 2$ represents a zero-holed torus, or sphere, $\chi_E = 0$ a one-holed torus, or doughnut, $\chi_E = -2$ a two-holed torus, and $\chi_E = 2-2N_E$ an N_E-holed torus. The tori shown in Fig. 7 (a–d) correspond to $\chi_E = 2, 0, -2$ and -4, respectively.

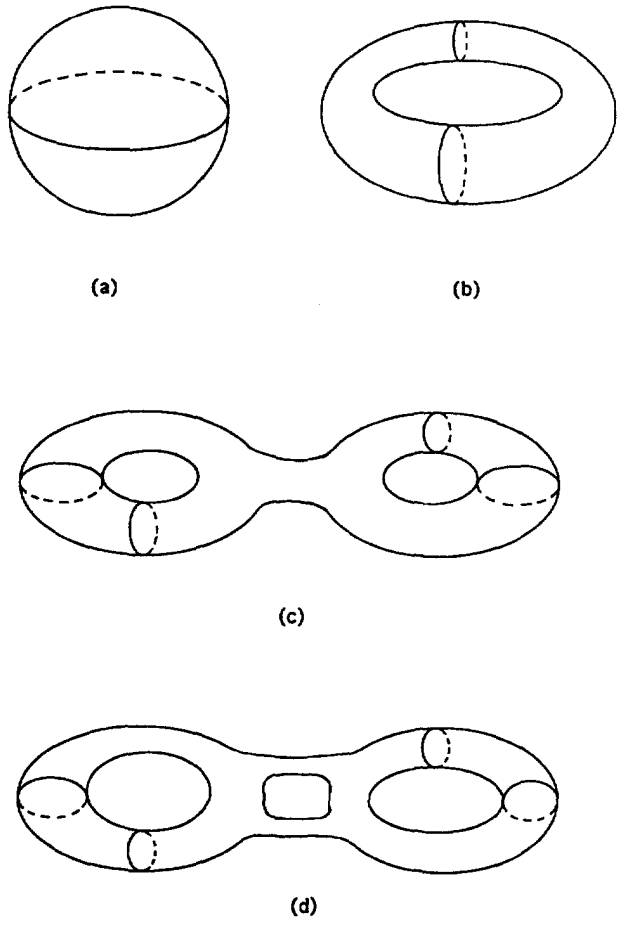

Fig. 7. The tori with the different Euler characteristics. (a) A sphere. (b) A doughnut. (c) A two-holed torus. (d) A three-holed torus.

In the present research, a simply connected plane is represented by the map of a one-holed torus instead of a sphere. In contrast with the map of a sphere on a projective plane showing only a half-sphere, this representation exhibits the whole view of a one-holed torus. Additionally, on the Euclidean plane, the torus map is a square or a quadrilateral instead of a circular map of a sphere and, therefore, it should be more convenient for treatments of experimental data. Meanwhile, the plane map for a many-holed torus is a consistent extension of the map of a one-holed torus.

The torus map of a one-holed torus

The map of a one-holed torus is made by plotting latitude θ and longitude ϕ of the torus shown in Fig. 8(a) as rectangular coordinates in a plane shown in Fig. 8(b). Because

$$-\pi < \theta \leqslant \pi, \quad -\frac{\pi}{2} \leqslant \phi \leqslant \frac{3\pi}{2}, \tag{2}$$

the map is a rectangular area which includes the top and right edges but not the bottom and left edges. A heavy line in Fig. 8(b) denotes an edge included in the map, whereas a light line indicates an edge not included. The solid dot represents a vertex included; a small circle stands for one not included. Each point on the torus has a unique image on the map. The torus map in Fig. 9 illustrates the subdivision of a simply connected plane into 17 triangles, two pentagons and five hexagons with only four-ordered and six-ordered vertices. The number given within a polygon refers to the number of its edges. It is easily seen that $N_0 = 21$, $N_1 = 45$ and $N_2 = 24$, and these numbers satisfy the Euler equation $\chi_E = 0$.

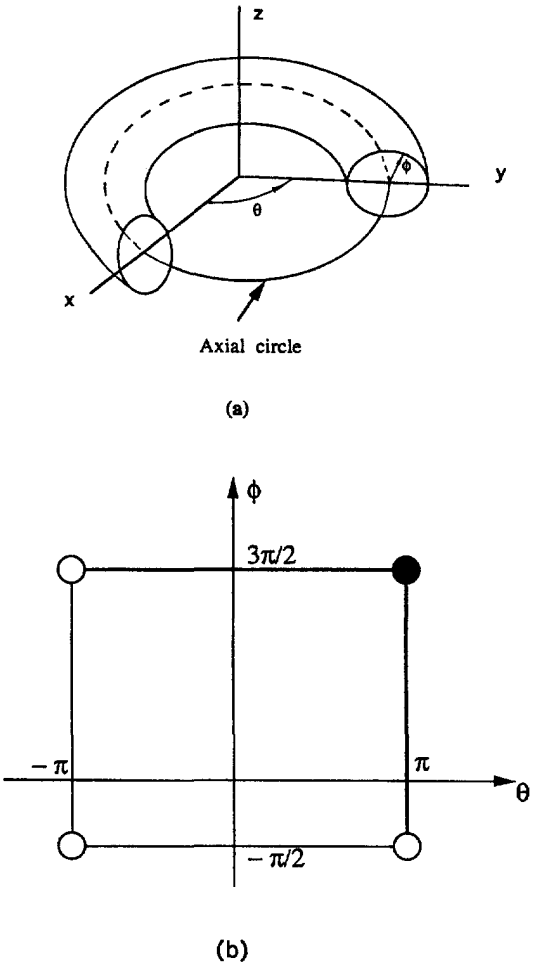

Fig. 8. (a) Illustration of constructing a torus map from a one-holed torus. (b) A torus map representing a simply connected plane.

The torus map of a two-holed torus

A torus map for a two-holed torus must now be introduced in some detail to meet the need of analysis of inhomogeneity. The torus map of a many-holed torus can be built by a similar process. As shown in Fig. 10(a), we first divide a two-holed torus into two one-holed tori by cutting the common tube shared by two annular surfaces. As a result, each one-holed torus contains a shadow defect resulted from the cut shown in Fig. 10(b). Second, a suitable latitude angle and longitude angle are introduced as before for either one of the two one-holed tori, and then a plane square with a shadow defect is plotted as shown in Fig. 11(a). The shadow defect on the map is defined as an inhomogeneous cell and it will not be counted as a normal cell in the follow-up subdivision of the map. One should bear in mind that the segments of boundary of an inhomogeneous cell are shared by polygons as their edges. The above cutting operation leads to two one-holed tori and hence two identical maps with the cells. Analysis of the subdivision of a plane needs only one, so the other one is simply treated as an identical image. Consequently, the Euler equation (1) for the subdivision of a multily-connected plane has the form

$$N_0 - N_1 + N_2 = \frac{\chi_E}{2} = 1 - N_E, \quad N_E > 1. \tag{3}$$

The proof of eqn (3) is not difficult, and is omitted here. When $N_E = 2$, eqn (3) corresponds to the map of owning one inhomogeneous cell; and when $N_E = 3$, it holds for the map of

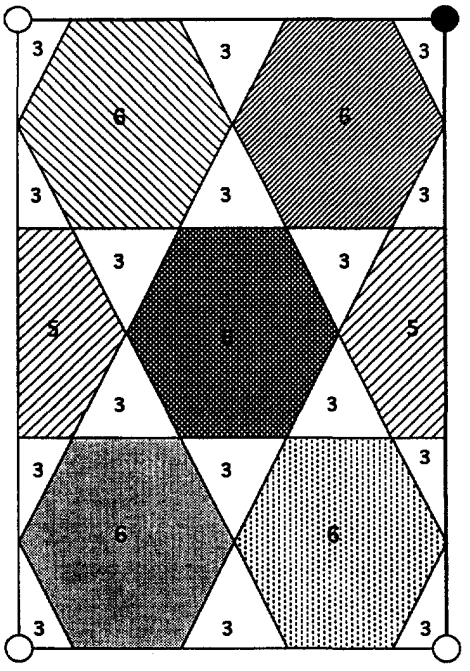

Fig. 9. An example for the subdivision of a simply connected plane.

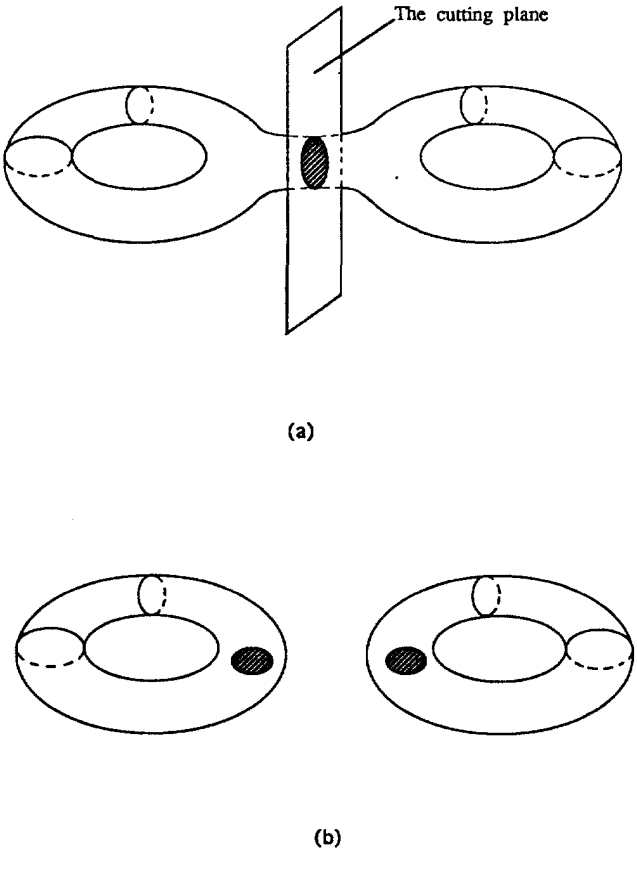

Fig. 10. Illustration of constructing a torus map with an inhomogeneous cell. (a) The cutting procedure. (b) Two one-holed tori with inhomogeneous cells.

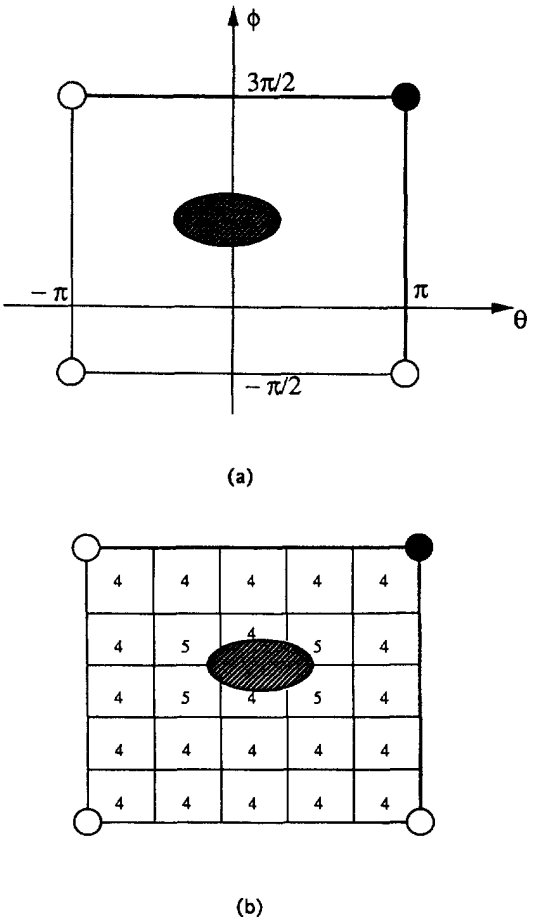

Fig. 11. An example for the subdivision of a multiply connected plane.

two inhomogeneous cells and so on. In the analogy of this, the number Θ of inhomogeneous cells on a map is determined by

$$\Theta = N_E - 1, \quad N_E > 1. \tag{4}$$

It is worth pointing out that the above cutting operation is not unique. Alternative operations may be found, but the current one appears to be most convenient for applications. An example for the subdivision of a square with an inhomogeneous cell is given in Fig. 11(b), containing 21 four-edged and four five-edged polygons. The numbers $N_0 = 29$, $N_1 = 55$ and $N_2 = 25$ satisfy the Euler equation (3) of $\chi_E = -2$ or $\Theta = 1$.

It should be noted that the size and shape of a polygon are heavily influenced by physical and/or biological parameters, especially for non-skeletal networks. For instance, the size and shape of a fragment depends on strain rate and energy balance (e.g. Lankford and Blanchard, 1991; Yong *et al.*, 1994); the average area of an n-sided metallurgical grain is controlled by free energy (e.g. Atkinson, 1988; Frost *et al.*, 1990) or temperature changes (Alles *et al.*, 1993); and the size of rat-liver cells is sensitive to chemical stain (Paiement, Dominguez and Messier, 1992). In addition, such examinations have also shown that the edge number of a polygon depends on its size and shape. Thus, it is reasonable to assume that physical and/or biological factors can only make contributions, if any, to the formation of three-edged and/or four-edged polygons. It will be proved that after the number of the two types of polygon is known, three fundamental equations derived next give a quantitative description to the other important parameters of a surface network.

3. FORMULATION

As discussed above, the torus map of a one-holed torus related to $\chi_E = 0$ can be used to represent a simply connected plane. Thus it is feasible by means of eqn (4) to write eqns (1) and (3) in the unified form

$$N_0 - N_1 + N_2 = -\Theta, \tag{5}$$

$$\Theta = N_E - 1, \quad N_E \geqslant 1, \tag{6}$$

for the subdivision of either simply connected or multiply connected surfaces. The main difference between eqns (1) and (5) is that eqn (5) is suitable for a generalized plane with inhomogeneous defects instead of a closed surface.

A dynamic process may change the values of N_0, N_1 and N_2 at an instant. However, the time-dependent rearrangements have no influence on the form of the Euler equation because it is a geometric equation. This feature of eqn (5) ensures that formulae derived from it are adaptable for dynamic models. The reason for this time-invariant property is that the increments of N_0, N_1 and N_2 are always in a self-equilibrium state. Here is the proof for this statement. After the time increment Δt, $N_i (i = 0, 1, 2)$ and Θ are altered to $N_i^*$and Θ^*, where

$$N_i^* = N_i + \frac{dN_i}{dt}\Delta t \quad (i = 0, 1, 2) \quad \text{and} \quad \Theta^* = \Theta + \frac{d\Theta}{dt}\Delta t. \tag{7}$$

dN_i/dt and $d\Theta/dt$ are the increasing rates of N_i and Θ, respectively. In the light of $N_0^* - N_1^* + N_2^* = -\Theta^*$ and eqns (5) and (7), one obtains

$$\frac{dN_0}{dt} - \frac{dN_1}{dt} + \frac{dN_2}{dt} = -\frac{d\Theta}{dt}. \tag{8}$$

Equation (8) can also be achieved by directly differentiating eqn (5) with respect to t. But the kinematic meaning of the Euler equation could be covered by such a procedure.

Without loss of generality, suppose that the subdivision of a plane into a network consists of n types of polygon with edges $k_1 < k_2 < \ldots < k_i < \ldots < k_n$ and m types of vertex with orders $j_1 < j_2 < \ldots < j_i < \ldots < j_m$. Meanwhile, the total number of polygons with edge k_i is denoted by K_i and the total number of vertices with order j_i is denoted by J_i. Since one edge connects two vertices and two polygons share one common edge, an ordinary geometric analysis leads to the following identities

$$2N_1 = \sum_{i=1}^{m} j_i J_i, \tag{9}$$

$$2N_1 = \sum_{i=1}^{n} k_i K_i + \sum_{i=1}^{\Theta} H_i, \tag{10}$$

$$N_0 = \sum_{i=1}^{m} J_i, \tag{11}$$

$$N_2 = \sum_{i=1}^{n} K_i, \tag{12}$$

where H_i is the edge number of the ith inhomogeneous cell.

For a general subdivision, there is no reason to exclude any type of polygon and any type of vertex unless an abnormal situation is specified. Therefore, it is natural to introduce the following iterative equations

$$j_{i+1} = 1+j_i = i+j_1 \quad (i = 1,2,\ldots,m-1), \tag{13}$$

$$k_{i+1} = 1+k_i = i+k_1 \quad (i = 1,2,\ldots,n-1). \tag{14}$$

It is very important to notice that neither eqn (13) nor (14) is a geometric constraint of the subdivision. Actually, if a network does not have a type of vertex and/or a type of polygon, for example, j_s and/or k_t where s and t are integers and $1 \leqslant s \leqslant m$, $1 \leqslant t \leqslant n$, one can take $J_s = 0$ and/or $K_t = 0$ for eliminating j_s and/or k_t.

Substitution of eqn (13) into eqn (9) yields

$$2N_1 = j_1 \sum_{i=1}^{m} J_i + \sum_{i=1}^{m-1} iJ_{i+1} = j_1 N_0 + \sum_{i=1}^{m-1} iJ_{i+1}. \tag{15}$$

Similarly, inserting eqn (14) into eqn (10) results in

$$2N_1 = k_1 \sum_{i=1}^{n} K_i + \sum_{i=1}^{n-1} iK_{i+1} + \sum_{i=1}^{\Theta} H_i = k_1 N_2 + \sum_{i=1}^{n-1} iK_{i+1} + \sum_{i=1}^{\Theta} H_i. \tag{16}$$

Adding eqn (15) to eqn (16) gives

$$4N_1 - k_1 N_2 - j_1 N_0 = \sum_{i=1}^{m-1} iJ_{j+1} + \sum_{i=1}^{n-1} iK_{i+1} + \sum_{i=1}^{\Theta} H_i \tag{17}$$

and then

$$4(N_1 - N_2 - N_0) + (4-k_1)N_2 + (4-j_1)N_0 = \sum_{i=1}^{m-1} iJ_{i+1} + \sum_{i=1}^{n-1} iK_{i+1} + \sum_{i=1}^{\Theta} H_i. \tag{18}$$

According to the Euler equation (5), eqn (18) becomes

$$(4-k_1)N_2 + (4-j_1)N_0 = -4\Theta + \sum_{i=1}^{m-1} iJ_{i+1} + \sum_{i=1}^{n-1} iK_{i+1} + \sum_{i=1}^{\Theta} H_i. \tag{19}$$

Equation (19) is one of the three fundamental formulae for analysis of topological constraints on surface networks. The other two are derived below.

Subtracting eqn (15) from eqn (16) produces

$$j_1 N_0 + \sum_{i=1}^{m-1} iJ_{i+1} = k_1 N_2 + \sum_{i=1}^{n-1} iK_{i+1} + \sum_{i=1}^{\Theta} H_i. \tag{20}$$

Equation (20) is rearranged into two forms

$$j_1(N_0 - N_1 + N_2) + \sum_{i=1}^{m-1} iJ_{i+1} = k_1 N_2 + j_1(N_2 - N_1) + \sum_{i=1}^{n-1} iK_{i+1} + \sum_{i=1}^{\Theta} H_i \tag{21}$$

and

$$j_1 N_0 + k_1(N_0 - N_1) + \sum_{i=1}^{m-1} iJ_{i+1} = k_1(N_2 - N_1 + N_0) + \sum_{i=1}^{n-1} iK_{i+1} + \sum_{i=1}^{\Theta} H_i. \tag{22}$$

In terms of the Euler equation (5), eqns (21,22) are simplified to

$$\sum_{i=1}^{m-1} iJ_{i+1} = j_1\Theta + k_1N_2 + j_1(N_2 - N_1) + \sum_{i=1}^{n-1} iK_{i+1} + \sum_{i=1}^{\Theta} H_i \tag{23}$$

and

$$\sum_{i=1}^{n-1} iK_{i+1} = k_1\Theta + j_1N_0 + k_1(N_0 - N_1) + \sum_{i=1}^{m-1} iJ_{i+1} - \sum_{i=1}^{\Theta} H_i. \tag{24}$$

Because of

$$N_2 - N_1 = \left(1 - \frac{k_1}{2}\right)N_2 - \frac{1}{2}\sum_{i=1}^{n-1} iK_{i+1} - \frac{1}{2}\sum_{i=1}^{\Theta} H_i \tag{25}$$

and

$$N_0 - N_1 = \left(1 - \frac{j_1}{2}\right)N_0 - \frac{1}{2}\sum_{i=1}^{m-1} iJ_{i+1}, \tag{26}$$

eqns (23, 24) are converted to

$$\sum_{i=1}^{m-1} iJ_{i+1} = j_1\Theta + \left[j_1 + k_1\left(1 - \frac{j_1}{2}\right)\right]N_2 + \left(1 - \frac{j_1}{2}\right)\sum_{i=1}^{n-1} iK_{i+1} + \left(1 - \frac{j_1}{2}\right)\sum_{i=1}^{\Theta} H_i \tag{27}$$

and

$$\sum_{i=1}^{n-1} iK_{i+1} = k_1\Theta + \left[k_1 + j_1\left(1 - \frac{k_1}{2}\right)\right]N_0 + \left(1 - \frac{k_1}{2}\right)\sum_{i=1}^{m-1} iJ_{i+1} - \sum_{i=1}^{\Theta} H_i. \tag{28}$$

Equations (27, 28) are the other two fundamental formulae. One may find other alternative equations through different approaches, but they are likely to be the linear combination of eqns (19) and (27, 28).

An important application of eqns (19) and (27–28) is that they reveal the symmetry between vertices and polygons of a general surface network. From the geometric point of view alone, it is unnecessary to distinguish the difference caused by physical inhomogeneity. As a result, Θ is taken as zero and $H_i (1 \leqslant i \leqslant \Theta)$ disappears from eqns (19) and (27, 28). In addition, a general surface network should possess both three-ordered vertices and three-edged polygons. After substitution of $j_1 = 3$ and $k_1 = 3$ into eqn (19), by using identities (9–12) and the Euler equation of $\Theta = 0$, one obtains

$$3J_1 + 2J_2 + J_3 = \sum_{i=1}^{m-4} iJ_{i+4} + 2\sum_{i=1}^{n-1} iK_{i+1} \tag{29}$$

and

$$3K_1 + 2K_2 + K_3 = \sum_{i=1}^{n-4} iK_{i+4} + 2\sum_{i=1}^{m-1} iJ_{i+1}, \tag{30}$$

respectively. Meanwhile, further analysis to eqns (29, 30) gives

$$4J_1 + 3J_2 + 2J_3 + J_4 = N_0 + \sum_{i=1}^{m-5} iJ_{i+5} + 2\sum_{i=1}^{n-1} iK_{i+1} \tag{31}$$

and

$$4K_1+3K_2+2K_3+K_4 = N_2+\sum_{i=1}^{n-5} iK_{i+5}+2\sum_{i=1}^{m-1} iJ_{i+1}. \tag{32}$$

In a similar fashion, eqns (29, 30) or (31, 32) can also be derived from eqns (27, 28). Equations (29, 30) and (31, 32) demonstrate that there is the symmetry between J_i and K_i. That is, after an orderly reciprocal exchange between vertices and polygons, the geometric constraints of a surface network remain unchanged. Mathematically speaking, if a pair of point sets $(\mathbf{J};\mathbf{K})$, where $\mathbf{J} = \{J_1, J_2, \ldots, J_m\}$ and $\mathbf{K} = \{K_1, K_2, \ldots, K_n\}$ satisfies constraints (29, 30), then the other pair of point sets $(\mathbf{K};\mathbf{J})$ given by

$$(\mathbf{K};\mathbf{J}) = (\mathbf{J};\mathbf{K}), \tag{33}$$

also satisfies eqns (29, 30) and it is symmetric to $(\mathbf{J};\mathbf{K})$.

Before discussions of specific cases, three simple examples for $\Theta = 0$ are given to illustrate how constraints are imposed on a surface network by eqns (19) and (27, 28) through the minimum-ordered vertices and the minimum-edged polygons.

(a) $k_1 = 6, j_1 = 3$. Either eqn (27) or (28) yields

$$2\sum_{i=1}^{m-1} iJ_{i+1} = -\sum_{i=1}^{n-1} iK_{i+1}.$$

Obviously, the only choice for both J_{i+1} and K_{i+1} is

$$J_{i+1} = 0, \quad 1 \leqslant i \leqslant m-1; \quad K_{i+1} = 0, \quad 1 \leqslant i \leqslant n-1.$$

It follows that on a network, if the edge number of a minimum-edged polygon is six and the order number of a minimum-ordered vertex is three, then the network is not allowed to have any other types of polygon and vertex due to geometric restrictions.

(b) $k_1 = 4, j_1 = 4$. Eqn (19) provides

$$\sum_{i=1}^{m-1} iJ_{i+1}+\sum_{i=1}^{n-1} iK_{i+1} = 0,$$

leading to

$$J_{i+1} = 0, \quad 1 \leqslant i \leqslant m-1; \quad K_{i+1} = 0, \quad 1 \leqslant i \leqslant n-1.$$

A conclusion similar to (a) can be drawn. On a surface network, if the minimum-edged polygon has four edges and the minimum-ordered vertex has order four, then the network is not allowed to have any other types of polygon and vertex.

(c) $k_1 = 3, j_1 = 6$. Either eqn (27) or (28) gives

$$\sum_{i=1}^{m-1} iJ_{i+1} = -2\sum_{i=1}^{n-1} iK_{i+1}$$

and thus

$$J_{i+1} = 0, \quad 1 \leqslant i \leqslant m-1; \quad K_{i+1} = 0, \quad 1 \leqslant i \leqslant n-1.$$

Obviously, on a network, if the minimum-edged polygon has three edges and the minimum-ordered vertex has order six, then the network is not allowed to have any other types of

polygon and vertex. The results for examples (a–c) are three well-known regular subdivisions of a simply connected plane. Any other subdivisions are called irregular subdivisions. They show that a surface network can be controlled completely by the minimum-edged polygons and the minimum-ordered vertices. In the next section, it will be verified that the minimum order of vertices is not an independent parameter, but controlled by the minimum edge of polygons, and vice versa.

From the point of symmetry, example (b) is a self-symmetric network; examples (a) and (c) are symmetric with each other. In fact, (c) can be derived from (a) by use of relation (33)

$$(\mathbf{J};\mathbf{K}) = (\{K_4\};\{J_1\}) = (\mathbf{K};\mathbf{J}) = (\{J_4\};\{K_1\}). \tag{34}$$

To simulate the failure of thin elastic films, Meakin (1988) designed a plane uniform skeletal network with triangular elastic bonds and six-ordered nodes which is mathematically coincident with example (c). Surprisingly, the final crack patterns obtained by Meakin (1988) are very close to the structure of example (a). It implies, in a topological sense, that to some extent a macroscopic crack pattern is the symmetric structure of a microscopic material arrangement as described by eqn (34).

4. APPLICATIONS

To have a better understanding of the analytical procedure adopted above, attention now focuses on the subdivision of a simply connected plane. Mathematically, this corresponds to $\Theta = 0$. Physically, the results obtained are applicable for a homogeneous network. The effects of inhomogeneous defects will be analyzed in the second part of this research. Because the different minimum edges of polygons have distinct consequences, detailed discussions into each case are given individually.

(i) $k_1 > 4$

Equation (19) for $k_1 > 4$ is rewritten as

$$(4-j_1)N_0 = (k_1-4)N_2 + \sum_{i=1}^{m-1} iJ_{i+1} + \sum_{i=1}^{n-1} iK_{i+1}. \tag{35}$$

Clearly, the only meaningful value of j_1 for eqn (35) is three. Therefore eqn (35) becomes

$$N_0 = (k_1-4)N_2 + \sum_{i=1}^{m-1} iJ_{i+1} + \sum_{i=1}^{n-1} iK_{i+1}. \tag{36}$$

After substitution of $j_1 = 3$ into eqn (27), one gains

$$\sum_{i=1}^{m-1} iJ_{i+1} = \left(3-\frac{k_1}{2}\right)N_2 - \frac{1}{2}\sum_{i=1}^{n-1} iK_{i+1}. \tag{37}$$

It is obvious from eqn (37) that there exist no meaningful results for $k_1 \geqslant 7$. In addition, the case of $k_1 = 6$ is the repetition of a regular subdivision which has been discussed in example (a) of Section 3. By the way, an exception discussed by Klamkin and Liu (1980) and Fulton (1992) for tessellations is not applicable here, since a very irregular pattern boundary is required. As a result, the only meaningful choice of $k_1 > 4$ is $k_1 = 5$. Inserting $k_1 = 5$ into eqn (37) results in

$$K_1 = \sum_{i=1}^{n-2} iK_{i+2} + 2\sum_{i=1}^{m-1} iJ_{i+1}. \tag{38}$$

Note that K_1 is independent of K_2 and J_1. Equation (38) shows that five-edged polygons

are convertible with polygons with more than six edges and vertices with order greater than three. If K_1 is given, then the upper limits of others are determined, for instance, $K_{i+2} \leqslant K_1/i$ and $J_{i+1} \leqslant K_1/2i$. Clearly, the greater the edge number of a polygon, the less the number of this type of polygon. The same conclusion holds for vertices. Furthermore, in a kinematic sense, the increasing rate of K_1 is of the form

$$\frac{dK_1}{dt} = \sum_{i=1}^{n-2} i\frac{dK_{i+2}}{dt} + 2\sum_{i=1}^{m-1} i\frac{dJ_{i+1}}{dt}, \tag{39}$$

in particular, giving

$$\frac{dK_{i+2}}{dt} \leqslant \frac{1}{i}\frac{dK_1}{dt} \quad \text{and} \quad \frac{dJ_{i+1}}{dt} \leqslant \frac{1}{2i}\frac{dK_1}{dt}. \tag{40}$$

Inequality (40) means that the maximum increasing rate of $(i+6)$-edged polygons is less than one-ith of the increasing rate of five-edged polygons. For $(i+3)$-ordered vertices, the maximum increasing rate reduces to one-$2i$th.

By making use of identity (11), $k_1 = 5$ and $j_1 = 3$, eqn (28) yields

$$J_1 = \frac{2}{3}N_0 + \sum_{i=1}^{m-2} iJ_{i+2} + \frac{2}{3}\sum_{i=1}^{n-1} iK_{i+1}. \tag{41}$$

The geometric meaning of eqn (41) is that if five-edged polygons act as the minimum-edged polygons in a surface network, then the number of three-ordered vertices is automatically larger than two-thirds of the total number of vertices in this network. No more conditions need be imposed to this conclusion. In this case, physical mechanisms, if any, do not make any significant contributions to the formation of three-ordered vertices, but prevent the appearance of four-edged and/or three-edged polygons from the surface network. In terms of eqns (11) and (41), this statement is also verified from another aspect by

$$\sum_{i=1}^{m-1} iJ_{i+1} = \frac{1}{3}N_0 - \frac{2}{3}\sum_{i=1}^{n-1} iK_{i+1}. \tag{42}$$

That is, the sum of all other types of vertex is much less than one-third of total vertices.

According to eqn (13), the maximum order j_m where $j_m = j_1 + m - 1$ can be determined when integer m is known. Thus, the first step is to evaluate m. Assume that none of J_{i+1} $(1 \leqslant i \leqslant m-1)$ and K_{i+3} $(1 \leqslant i \leqslant n-3)$ is equal to zero, and then an inequality for m is derived from eqn (38) in the form

$$m(m-1) \leqslant \frac{1}{J_{\min(m-1)}}[K_1 - K_3 - \tfrac{1}{2}n(n-3)K_{\min(n-3)}] \tag{43}$$

and it yields

$$j_m < j_m^u = j_1 + \sqrt{K_1 - K_3 + \tfrac{1}{4}} - \tfrac{1}{2} \tag{44}$$

due to

$$\begin{aligned} m &\leqslant \sqrt{\frac{1}{J_{\min(m-1)}}[K_1 - K_3 - \tfrac{1}{2}n(n-3)K_{\min(n-3)}] + \tfrac{1}{4}} + \tfrac{1}{2} \\ &\leqslant \sqrt{K_1 - K_3 - \tfrac{1}{2}n(n-3) + \tfrac{1}{4}} + \tfrac{1}{2} < \sqrt{K_1 - K_3 + \tfrac{1}{4}} + \tfrac{1}{2}, \end{aligned}$$

where $m \geqslant 2$ and $n \geqslant 4$. Here j_m^u is an upper limit of j_m, $K_{\min(n-3)} \geqslant 1$ is the minimum value of the set $\{K_4, K_5, \ldots, K_n\}$ and $J_{\min(m-1)} \geqslant 1$ is the minimum value of the set $\{J_2, J_3, \ldots, J_m\}$. Similarly, the estimation for the maximum edge k_n, where $k_n = k_1 + n - 1$ is also available from eqn (14) if n is given. Based on eqn (38), an inequality for k_n is given by

$$k_n < k_n^u = k_1 + \sqrt{2(K_1 - K_3) + \tfrac{9}{4}} + \tfrac{1}{2}, \tag{45}$$

since

$$\begin{aligned} n &\leqslant \sqrt{\frac{2}{K_{\min(n-3)}}[K_1 - K_3 - m(m-1)J_{\min(n-1)}] + \tfrac{9}{4}} + \tfrac{3}{2} \\ &\leqslant \sqrt{2(K_1 - K_3) - m(m-1) + \tfrac{9}{4}} + \tfrac{3}{2} < \sqrt{2(K_1 - K_3) + \tfrac{9}{4}} + \tfrac{3}{2}, \end{aligned}$$

with $m \geqslant 2$ and $n \geqslant 4$. Here k_n^u is an upper limit of k_n. Note that one of the two maximum parameters, j_m^u and k_n^u, increases with the decrease of the other one.

Owing to smaller upper limit j_m^u, the generation of high-ordered vertices is more difficult than the generation of high-edged polygons. This is possibly a main reason for the frequent appearance of high-edged polygons and the absence of high-ordered vertices in natural and random artificial surface networks. More accurate estimation for both j_m^u and k_n^u can be conducted by adding more terms into eqns (44) and (45). By the way, $J_{i+1} \neq 0$ $(1 \leqslant i \leqslant m-1)$ and $K_{i+3} \neq 0$ $(1 \leqslant i \leqslant n-3)$ are dispensable conditions. They are introduced simply for the convenience of derivations and can be removed if necessary.

During the collection of experimental data for verification of theoretical models, one could encounter great difficulties caused by constructing an exact torus map. This kind of difficulty is also unavoidable for classical models (Smith, 1952). To alleviate this situation, an alternative method is suggested here. Application of eqn (12) to eqn (38) yields

$$4K_1 + 3K_2 + 2K_3 + K_4 = 3N_2 + \Delta R \tag{46}$$

where

$$\Delta R = \sum_{i=1}^{n-5} iK_{i+5} + 2\sum_{i=1}^{m-1} iJ_{i+1}.$$

To be close to an exact torus map as accurately as possible, the polygons given within a square or a quadrilateral area are counted, and, most importantly, the numbers of both polygons and vertices on one side of boundaries should be close or, if possible, equal to these on its opposite side. In such circumstances, the only error source of experimental data is the mismatched parts of boundary polygons and vertices, and it is independent of size of pattern. If ΔR is negligibly small or equal to zero, then eqn (46) yields a brief expression of N_2

$$N_2^A = \tfrac{1}{3}(4K_1 + 3K_2 + 2K_3 + K_4), \tag{47}$$

where N_2^A denotes the experimental value of N_2 with the potential error. Note that N_2^A relies only on low-edged polygons, and hence the collecting process of experimental data becomes very convenient. Sometimes, the accuracy of N_2^A can be improved by adding more terms, including J_{i+1}, to eqn (47) if ΔR is not negligible.

Because three inequalities $J_1 \geqslant 2/3N_2$, $k_n < k_n^u$ and $j_m < j_m^u$ are so obvious in the surface networks collected, their experimental verifications are not listed here. In this paper, all the experimental data but one for bubbles (Aboav, 1980) are obtained by the author through observations on a variety of surface networks.

(1) A coat pattern of a giraffe (Dagg and Forster, 1976; see Fig. 2 of this paper). A four-edged polygon in the middle of its neck is not counted.

$$K_1 = 12, \quad K_2 = 11, \quad K_3 = 4, \quad K_5 = 1, \quad \text{other polygons} = 0;$$

$$N_2 = 28, \quad N_2^A = 30, \quad \Delta N_2 = 7.1\%,$$

where ΔN_2 denotes the percentage error of N_2.

(2) A bubble pattern (Aboav, 1980, p. 47, table 1).

$$K_1 = 580, \quad K_2 = 3511, \quad K_3 = 516, \quad K_4 = 5, \quad \text{others} = 0;$$

$$N_2 = 4612, \quad N_2^A = 4630 \quad \Delta N_2 = 0.39\%.$$

(3) A biological cellular network (Schejter and Wieschaus, 1993, p. 374, fig. 1j).

$$K_1 = 4, \quad K_2 = 16, \quad \text{others} = 0;$$

$$N_2 = 20, \quad N_2^A = 21, \quad \Delta N_2 = 5.0\%.$$

(4) A borosilicate grain pattern (Selleck *et al.*, 1990, p. 83, fig. 1D). A four-edged grain at the upper right corner is not counted.

$$K_1 = 10, \quad K_2 = 7, \quad K_3 = 1, \quad K_4 = 1, \quad K_6 = 1, \quad \text{others} = 0;$$

$$N_2 = 20, \quad N_2^A = 21, \quad \Delta N_2 = 5.0\%.$$

(ii) $k_1 = 4$

Equation (19) for $k_1 = 4$ and $\Theta = 0$ is of the form

$$(4-j_1)N_0 = \sum_{i=1}^{m-1} iJ_{i+1} + \sum_{i=1}^{n-1} iK_{i+1}. \tag{48}$$

Obviously, eqn (48) holds only for $j_1 = 3$ or $j_1 = 4$. The case of $j_1 = 4$ has been discussed in example (b) of Section 3. Thus, the only meaningful value of j_1 is $j_1 = 3$. In terms of identity (11), eqn (48) is written as

$$J_1 = \sum_{i=1}^{m-2} iJ_{i+2} + \sum_{i=1}^{n-1} iK_{i+1}. \tag{49}$$

Equation (49) shows that three-ordered vertices are much more than the sum of all other types of vertex except for four-ordered vertices.

Substitution of $k_1 = 4$ and $j_1 = 3$ into eqn (27) of $\Theta = 0$ obtains

$$N_2 = \frac{1}{2}\sum_{i=1}^{n-1} iK_{i+1} + \sum_{i=1}^{m-1} iJ_{i+1}. \tag{50}$$

By means of identity (12), eqn (50) is converted to

$$2K_1 + K_2 = \sum_{i=1}^{n-3} iK_{i+3} + 2\sum_{i=1}^{m-1} iJ_{i+1}. \tag{51}$$

Again, eqn (51) indicates that many-edged polygons and many-ordered vertices are convertible only with low-edged polygons, namely, four-edged and five-edged polygons. Based on eqns (49) and (51), another expression for J_1 is determined by

$$J_1 = \frac{2}{3}N_0 + \sum_{i=1}^{m-2} iJ_{i+2} + \frac{2}{3}\left(\sum_{i=1}^{n-2} iK_{i+2} - K_1\right). \tag{52}$$

Evidently, if

$$\sum_{i=1}^{n-2} iK_{i+2} \geqslant K_1, \tag{53}$$

then $J_1 \geqslant 2N_0/3$. Note that condition (53) is independent of K_2, the number of five-edged polygons. In a similar fashion, the formula for J_{i+1} is found by use of eqns (49) and (51) in the form

$$\sum_{i=1}^{m-1} iJ_{i+1} = \frac{1}{3}N_0 - \frac{2}{3}\left(\sum_{i=1}^{n-2} iK_{i+2} - K_1\right). \tag{54}$$

According to eqn (54), provided that eqn (53) does not hold, other types of vertex such as four-ordered vertices have potential to be more than one-third of the total vertices or even larger than that. Moreover, eqn (54) suggests that the traditional assumption about $J_{i+1} = 0$ $(i \geqslant 1)$ is a very special case since it requires

$$N_0 = J_1 = 2\left(\sum_{i=1}^{n-2} iK_{i+2} - K_1\right). \tag{55}$$

The appearance of four-edged polygons in eqn (52) provides an opportunity to physical parameters to make influences on inequality $J_1 \geqslant 2/(3N_0)$. However, their functions can be still limited to a small scope. When the number of any type of polygon with six or more edges is larger than a small fraction of four-edged polygons, for instance, $K_{i+2} \geqslant K_1/i (i \geqslant 1)$, inequality $J_1 \geqslant 2/(3N_0)$ retains. Meanwhile, if $K_2 \geqslant K_1$, that is, the number of five-edged polygons is greater than the number of four-edged polygons, while the distribution of other polygons are arbitrary, an estimation for J_1 is given from eqns (51) and (52) by

$$J_1 \geqslant \frac{2}{5}N_0 + \sum_{i=1}^{m-2} iJ_{i+2} + \frac{4}{5}\sum_{i=1}^{n-3} iK_{i+3} + \frac{6}{5}\sum_{i=1}^{n-2} K_{i+2}. \tag{56}$$

Still, in this case, more than 40% of the total number of vertices are three-ordered vertices.

When an opposite case $K_1 \geqslant K_{i+1} (i \geqslant 1)$ against $K_i \geqslant K_1$ occurs, is there any possibility of having $J_1 \geqslant 2/(3N_0)$? If the answer is positive, what is the critical value of a $K_i (i \geqslant 1)$? The critical values of $K_i (i = 1, 2, \ldots, n)$ are very important because once they are determined, researchers are capable of controlling the number of three-ordered vertices by adjusting the ratio of different polygons with respect to the total number of polygons. Let

$$\sum_{i=1}^{n-2} iK_{i+2} - K_1 = 0, \tag{57}$$

then eqn (52) yields

$$J_1 = \tfrac{2}{3}N_0 + \sum_{i=1}^{m-2} iJ_{i+2}. \tag{58}$$

Equation (57) is equivalent to the equation

$$K_1^c = \tfrac{1}{2}N_2 \tag{59}$$

if

$$\sum_{i=1}^{n-3} iK_{i+3} - K_2 = 0, \tag{60}$$

where K_1^c denotes the critical value of K_1. Hereinafter K_i^c $(i = 1, 2, \ldots, n)$ are used to represent the critical values of K_i. By repeating the same operation on eqn (60), one obtains

$$K_i^c = 2^{-i}N_2 \quad (i = 1, 2, \ldots, n-3), \tag{61}$$

$$K_{n-2}^c = K_n^c, \tag{62}$$

$$2K_{n-2}^c + K_{n-1}^c = K_{n-3}^c = 2^{-(n-3)}N_2. \tag{63}$$

The arrangement of polygons

$$\begin{aligned} \mathbf{K}^c &= \{K_1, K_2^c, \ldots, K_{n-2}^c, K_{n-1}^c, K_n^c\} \\ &= \left\{\frac{1}{2}N_2, \frac{1}{4}N_2, \ldots, \frac{N_2}{2^{n-3}}, K_{n-2}^c, K_{n-1}^c, K_n^c\right\} \end{aligned} \tag{64}$$

is called the critical distribution of polygons for the maintenance of $J_1 \geqslant 2/(3N_0)$. When $K_1 > N_2/2$, other reactions like $K_2^c < N_2/4$ or $K_3^c < N_2/8$ could lead to $J_1 < 2/(3N_0)$.

In terms of eqn (51), upper limits k_n^u and j_m^u are determined by

$$k_m < k_n^u = k_1 + \sqrt{2(2K_1 + K_2 - K_4) + \tfrac{9}{4}} + \tfrac{3}{2} \tag{65}$$

and

$$j_m < j_m^u = j_1 + \sqrt{2K_1 + K_2 - K_4 + \tfrac{1}{4}} - \tfrac{1}{2} \tag{66}$$

with $m \geqslant 2$ and $n \geqslant 5$. It follows from eqns (65) and (66) that four-edged and five-edged polygons are major factors to monitor upper limits k_n^u and j_m^u. Nevertheless, since K_1 has a larger weighting coefficient than K_2 does, four-edged polygons should more probably cause higher-edged polygons or higher-ordered vertices.

After the small parameters of eqn (51), compared with $5K_1 + 4K_2 + 3K_3 + 2K_4$, are neglected, experimental value N_2^A of N_2 is of the form

$$N_2^A = \tfrac{1}{3}(5K_1 + 4K_2 + 3K_3 + 2K_4). \tag{67}$$

The experimental verification for eqn (67) is listed below.

(1) A crack pattern (Meakin, 1988, p. 173, fig. 1d).

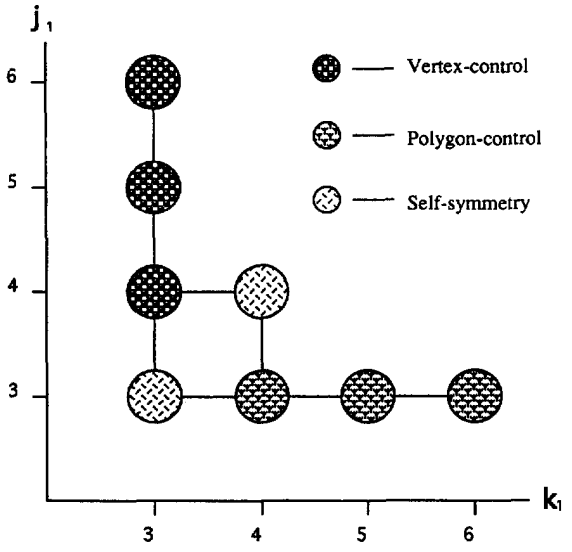

Fig. 12. A representation of symmetry of surface networks.

$$K_1 = 2, \quad K_2 = 8, \quad K_3 = 26, \quad K_4 = 4, \quad K_5 = 1, \quad \text{others} = 0;$$

$$N_2 = 41, \quad N_2^{\mathrm{A}} = 43, \quad \Delta N_2 = 4.5\%.$$

(2) A crack pattern shown in Fig. 3.

$$K_1 = 5, \quad K_2 = 12, \quad K_3 = 10, \quad K_4 = 4, \quad K_5 = 3, \quad \text{others} = 0;$$

$$N_2 = 34, \quad N_2^{\mathrm{A}} = 37, \quad \Delta N_2 = 8.8\%.$$

(3) A cellular network (Boitano, Dirksen and Sanderson, 1992, p. 294, fig. 2A).

$$K_1 = 3, \quad K_2 = 10, \quad K_3 = 20, \quad K_4 = 8, \quad \text{others} = 0;$$

$$N_2 = 41, \quad N_2^{\mathrm{A}} = 44, \quad \Delta N_2 = 7.3\%.$$

One reason for the high accuracy of N_2^{A} is that three-ordered vertices are the dominant majority in most surface networks. If $J_{i+1}(i \geqslant 1)$ or other terms of polygons truncated from eqn (67) are not negligible, their effects should be included.

(iii) $k_1 = 3$

In cases of $k_1 \geqslant 4$, i.e. the edge number of a minimum-edged polygon is more than or equal to four, regardless of two regular subdivisions, there is no choice for the value of the minimum-ordered vertex j_1 other than $j_1 = 3$. This kind of geometric constraint is here defined as polygon-control. According to symmetric property (33), the only choice of k_1 is $k_1 = 3$ if $j_1 \geqslant 4$. In this circumstance, the polygon-control is transmitted to vertex-control. All the formulae for $j_1 \geqslant 4$ can be obtained directly from formulae for $k_1 \geqslant 4$ by exchanging $J_i\,(i = 1, 2, \ldots, m)$ with $K_i\,(i = 1, 2, \ldots, n)$. The vertex-control will not be analyzed because of their rare appearance in non-skeletal surface networks. It should be noted that $k_1 = j_1 = 3$ is neither the case of polygon-control nor vertex-control. Indeed, it is a more complex self-symmetric structure in comparison with $j_1 = k_1 = 4$. A pictorial illustration is given in Fig. 12 for the symmetry of surface networks.

After subtraction of eqn (30) from eqn (31), further analysis leads to

$$J_1 = \frac{2}{3}N_0 + \sum_{i=1}^{m-2} iJ_{i+2} + \frac{2}{3}\left(\sum_{i=1}^{n-3} iK_{i+3} - 2K_1 - K_2\right). \tag{68}$$

The formula for $J_{i+1}(i \geqslant 1)$ is determined by

$$\sum_{i=1}^{m-1} iJ_{i+1} = \frac{1}{3}N_0 - \frac{2}{3}\left(\sum_{i=1}^{n-3} iK_{i+3} - 2K_1 - K_2\right). \tag{69}$$

It is apparent from eqn (68) that the theoretical basis of conventional models is the following identity

$$N_0 = J_1 = 2\left(\sum_{i=1}^{n-3} iK_{i+3} - 2K_1 - K_2\right) \tag{70}$$

in connection to $J_{i+1} = 0$ $(i = 1, 2, \ldots, m-1)$. Note that condition (70) is independent of five-edged polygons.

In terms of eqn (68), the ratio of the number of three-ordered vertices to the total number of vertices is more seriously affected due to the appearance of three-edged polygons. However, the dominant occupation of three-edged vertices among all the vertices can still retain if

$$\sum_{i=1}^{n-3} iK_{i+3} \geqslant 2K_1 + K_2 \tag{71}$$

where five-edged polygons are not contained, and hence K_3 is arbitrary. When $K_3 \geqslant 3K_1 + K_2$ and the distribution of other polygons is arbitrary, analysis into eqns (32) and (68) results in

$$J_1 \geqslant \frac{2}{5}N_0 + \sum_{i=1}^{m-2} iJ_{i+2} + \frac{2}{5}\sum_{i=1}^{n-4}(2i+3)K_{i+4} + \frac{6}{5}K_4. \tag{72}$$

This means that in this case $J_1 \geqslant 2/(5N_0)$. More deliberate examinations on eqns (32) and (68) lead to

$$J_1 \geqslant \frac{2\lambda-4}{3\lambda-4}N_0 + \sum_{i=1}^{m-2} iJ_{i+2} + \frac{2}{3\lambda-4}\sum_{i=1}^{n-4}[(i+1)\lambda - i]K_{i+4} \tag{73}$$

if

$$K_3 + \lambda K_4 \geqslant (2\lambda-3)K_1 + (\lambda-2)K_2, \tag{74}$$

where $\lambda \geqslant 2$. The synthetic influence of any two or more types of polygon on three-ordered vertices can be analyzed in a similar way.

By virtue of

$$\sum_{i=1}^{n-3} iK_{i+3} - 2K_1 - K_2 = 0, \tag{75}$$

certain calculations obtain the critical distribution $\mathbf{K}^c$ of polygons for $J_1 \geqslant 2/(3N_0)$,

$$\mathbf{K}^{\mathrm{c}} = \{K_1^{\mathrm{c}}, K_2^{\mathrm{c}}, \ldots, K_{n-4}^{\mathrm{c}}, K_{n-3}^{\mathrm{c}}, K_{n-2}^{\mathrm{c}}, K_{n-1}^{\mathrm{c}}, K_n^{\mathrm{c}}\}$$
$$= \left\{\frac{N_2}{3}, \frac{2N_2}{3^2}, \ldots, \frac{2^{n-5}}{3^{n-4}}N_2, 0, \frac{2^{n-5}}{3^{n-4}}N_2, 0, \frac{2^{n-5}}{3^{n-4}}N_2\right\}, \tag{76}$$

where

$$K_{n-3}^{\mathrm{c}} = K_{n-1}^{\mathrm{c}} = 0, \tag{77}$$

$$K_{n-2}^{\mathrm{c}} = K_n^{\mathrm{c}} = K_{n-4}^{\mathrm{c}} = \frac{2^{n-5}}{3^{n-4}}N_2. \tag{78}$$

According to the author's observations, there exist significant differences between many natural networks and the critical distribution. This may be of interest for applications because these differences can accommodate great variations of geometric structure of a material without loss of dominant occupation of three-ordered vertices. More importantly, this kind of geometric change could hopefully result in improvements of physical or biological behaviors of the material. From this point of view, eqn (76) provides a quantitative basis for the description of granular and biological materials.

Other formulas for case $j_1 = k_1 = 3$ are determined by

$$j_m < j_m^{\mathrm{u}} = j_1 + \sqrt{3K_1 + 2K_2 + K_3 - K_5 - 2J_2 + \tfrac{9}{4}} - \tfrac{1}{2}, \tag{79}$$

$$k_m < k_n^{\mathrm{u}} = k_1 + \sqrt{2(3K_1 + 2K_2 + K_3 - K_5 - 2J_2) + \tfrac{9}{4}} + \tfrac{5}{2}, \tag{80}$$

with $m \geqslant 3$ and $n \geqslant 6$, and

$$N_2^{\mathrm{A}} = \tfrac{1}{3}(6K_1 + 5K_2 + 4K_3 + 3K_4 + 2K_5 - 2J_2). \tag{81}$$

In the first time, the number J_2 of four-ordered vertices is taken into account for $j_m^{\mathrm{u}}, k_n^{\mathrm{u}}$ and N_2^{A} because in many cases it is not negligible for satisfactory accuracy. Some comparisons between N_2 and N_2^{A} are given below.

(1) A leaf-vein network shown in Fig. 3d. Only a part of the network is counted.

$$K_1 = 5, \quad K_2 = 34, \quad K_3 = 22, \quad K_4 = 23,$$

$$K_5 = 2, \quad K_6 = 0, \quad K_7 = 1; \quad J_2 = 38;$$

$$N_2 = 87, \quad N_2^{\mathrm{A}} = 95, \quad \Delta N_2 = 9.2\%.$$

(2) A ceramic grain array (Tuttle *et al.*, 1993, p. 1540, fig. 3A).

$$K_1 = 3, \quad K_2 = 13, \quad K_3 = 17, \quad K_4 = 18,$$

$$K_5 = 14, \quad K_6 = 1; \quad J_2 = 10;$$

$$N_2 = 66, \quad N_2^{\mathrm{A}} = 71, \quad \Delta N_2 = 7.6\%.$$

(3) A biological cellular pattern (Boudier *et al.*, 1993, p. 25, fig. 2a). Only a part of the network is counted.

$$K_1 = 1, \quad K_2 = 4, \quad K_3 = 14,$$

$$K_4 = 7, \quad K_5 = 2; \quad J_2 = 10;$$

$$N_2 = 28, \quad N_2^{\mathrm{A}} = 30, \quad \Delta N_2 = 7.1\%.$$

(4) A bubble arrangement (Aboav, 1980, p. 49, table 6).

$$K_1 = 20, \quad K_2 = 65, \quad K_3 = 170, \quad K_4 = 153,$$

$$K_5 = 87, \quad K_6 = 45, \quad K_7 = 19, \quad K_8 = 10,$$

$$K_9 = 6, \quad K_{10} = 6, \quad K_{11} = 2, \quad K_{16} = 1;$$

$$J_2 = 0 \quad N_2 = 584, \quad N_2^{\mathrm{A}} = 586, \quad \Delta N_2 = 0.3\%.$$

N_2^{A} is consistent with other four groups of experimental data given by Aboav (1980), where the maximum error is 2.1%. Other formulae, like eqns (68) and (79), are also in agreement with experimental results, but they are not given for the sake of brevity.

One more example is now given for illustrating how to apply topological constraints of surface networks to the analysis of a fragmentation problem. Assume that all the vertices of a crack network are three-ordered, and then eqn (15) gives $2N_1 = 3N_0$. In this case, the Euler equation reduces to

$$N_2 = -\Theta + \tfrac{1}{3}N_1, \tag{82}$$

where Θ denotes the number of defects of a solid material, such as cavities. In the analysis, the average area and length of fragments are expressed by a_0 and l_0, respectively. Based on eqn (82), applications of energy balance and geometric restrictions lead to the governing equation

$$\lambda_1(K_i)\frac{A_0}{a_0} = -\Theta + \frac{1}{3}\frac{\Delta E}{\lambda_2(K_i) l_0 \gamma_0} \tag{83}$$

for a_0 and l_0. In eqn (83), $\lambda_1(K_i)$ and $\lambda_2(K_i)$ are the weighting coefficients, A_0 is the total area of the fragmentation, γ_0 is the average density of surface energy and ΔE is the internal energy consumed by surface energy. For an adiabatic process, ΔE has the form

$$\Delta E = \int_{t_0}^{t} \mathrm{d}t \int_{A_0} \mathrm{tr}(\mathbf{TD})\,\mathrm{d}A, \tag{84}$$

where $\mathbf{T}$ is the stress tensor and $\mathbf{D}$ the stretching tensor. The relation between $\mathbf{T}$ and $\mathbf{D}$ depends on the constitute model of the material (Bowen, 1989). A detailed discussion into eqn (83) has been conducted by Yong (1994b).

5. DISCUSSION

Surface networks are an important part of either natural phenomena or scientific research. It is an interesting topic to reveal the underlying mechanisms of evolution and formation of a surface network. As a common phenomenon involved in analysis of geometric constraints, the formation of three-ordered vertices has long been contributed to direct effects of physical and/or biological parameters, such as the surface tension, despite the lack of sufficient experimental and theoretical proof. Although bubble arrangements and some other patterns, such as metallurgical grain arrays, are alike in vertex structures,

they differ remarkably in the formation process. Moreover, three-ordered vertices are also in the majority in many surface networks which show no existence of surface tension at all. A recent result obtained by Tuttle *et al.* (1993) demonstrate that there is a considerable number of four-ordered vertices associated with a fairly high ratio of four-edged grains in the $Pb(Zr, Ti)O_3$ film. Theoretical analysis and experimental verifications in the present research show that if an evolution process is relatively uniform, three-ordered vertices could result mainly from geometric constraints instead of a physical and biological consequence, because only a limited number of three-edged and/or four-edged polygons arise in networks. In other words, physical and/or biological parameters may play an assistant role under the domination of geometric constraints. For instance, they might contribute to the ratio of the number of three-edged and/or four-edged polygons to the total number of polygons.

Mathematically speaking, no matter how complex a surface network appears to be, there exists a simple symmetric relation between its vertices and polygons. Any variation of a surface network contains little mathematical surprise, rather than a kind of reciprocal transformation between vertices and polygons. Some assertions about asymmetric natures of surface networks (Weaire and Rivier, 1984) may need modifications. To a certain degree, three regular subdivisions serve as three centers of transmission between the vertex-control and the polygon-control. For example, when $k_1 = 4$, four-edged polygons and four-ordered vertices have potential to become the dominant majority of a surface network. In such circumstances, the variations of polygons and vertices take place between two regular subdivisions $(k_1; j_1) = (6; 3)$ and $(k_1; j_1) = (4; 4)$.

Encouraging information obtained in this work for applications is that the geometric structure of a surface network can be greatly rearranged without loss of the dominant share of three-ordered vertices in the network. It is expected that the large geometric variations could bring about significant improvements of physical and/or biological behavior of the network. At the first step, it seems easy to realize this idea by using computer simulation.

More examinations are needed for deep insight into all the mechanisms of evolution and formation of a surface network. Three-dimensional geometric constraints and thermodynamic effects are probably two important aspects for future work.

Acknowledgment—The author is grateful to Dr Dagg for her kind permission to reproduce the figure of the giraffe. The appreciation is extended to the reviewers for their insightful comments that led to improvement of this paper. The author would also like to thank Professor L. M. Brock for his helpful suggestions on the revision of the manuscript.

REFERENCES

Aboav, D. A. (1980). The arrangement of cells in a net. *Metalography* **13,** 43–58.

Alles, A. B., Puskas, R. P., Callaham, G. and Burdick, V. L. (1993). Compositional effects on the liquid-phase sintering of praseodymium oxide-based zinc oxide varistors. *J. Am. Ceram. Soc.* **76,** 2098–20102.

Anderson, M. P. and Rollett, A. D. (1990). *Simulation and Theory of Evolving Microstructures*. The Minerals, Metals & Materials Society.

Atkinson, H. V. (1988). Theories of normal grain growth in pure single phase systems. *Acta. Metall* **36,** 469–491.

Blackett, W. B. (1967). *Elementary Topology*. Academic Press, New York.

Boitano, S., Dirksen, E. R. and Sanderson, M. J. (1992). Intercellular propagation of calcium waves mediated by inositol trisphosphate. *Science* **258,** 292–295.

Boudier, J-A., Fantini, J., Gerard, C. and Verrivier, A. (1993). Polarized distribution of γ interferon-simulated MHC antigens and transferrin receptors in a clonal cell line isolated from Fisher rat thyroid (FRT Cells). *Cell Tissue Res.* **272,** 23–31.

Bowen, R. M. (1989). *Introduction Continuum Mechanics for Engineers*. Plenum Press, New York.

Dagg, A. I. and Foster, J. B. (1976). *The Giraffe—its Biology, Behavior and Ecology*. Van Nostrand Reinhold, New York.

Dormor, K. J. (1980). *Fundamental Tissue Geometry for Biologists*. Cambridge University Press, Cambridge.

Frost, H. J., Thompson, C. V. and Walton, D. T. (1990). Simulation of thin film grain growth structures—I. Grain growth stagnation. *Acta Metall.* **38,** 1455–1462.

Fulton, C. (1992). Tessellations. *Am. Math. Mthly* **99,** 442–445.

Glazier, J. A., Grest, G. S. and Anderson, M. P. (1990). "Ideal" two dimensional grain growth. In *Simulation and Theory of Evolving Microstructures* (Edited by M. P. Anderson and A. D. Rollett), pp. 41–45. The Minerals, Metals & Materials Society.

Klamkin, M. S. and Liu, A. (1980). Note on a result of Niven on impossible tessellations. *Am. Math. Mthly* **87,** 651–653.

Lankford, J. and Blanchard, C. R. (1991). Fragmentation of brittle materials at high rates of loading. *J. Mater. Sci.* **26,** 3067–3072.

Meakin, P. (1988). A simple model for elastic fracture in thin films. *Thin Solid Films* **151,** 165–190.
Meakin, P. (1991). Models for material failure and deformation. *Science* **252,** 226–234.
Murray, J. D. (1989). *Mathematical Biology*. Springer, Berlin.
Paiement, J., Dominguez, M. J. and Messier, P.-E. (1992). Cytoplasmic membrane transplants in early *Xenopus embryos indicate cell-cycle-specific effects*. *Biochem. Cell Biol.* **70,** 1290–1300.
Schejter, E. D. and Wieschaus, E. (1993). Bottleneck acts as a regulator of the microfilament network governing cellularization of the drosophila embryo. *Cell* **75,** 373–385.
Selleck, M. E., Rajan, K and M. E. Glicksman (1990). Organic materials as an experimental model. In *Simulation and Theory of Evolving Microstructures* (Edited by M. P. Anderson and A. D. Rollett), pp. 79–85. The Minerals, Metals & Materials Society.
Sleeper, B. (1993). And strips on the tail. *Pacific Disc.* **46,** 8–16.
Smith, C. S. (1952). Grain shapes and other metallurgical applications of topology. In *Metal Interfaces*. American Society for Metals, Cleveland, OH.
Thompson, D. W. (1963). *On Growth and Form*, I–II (first edition in 1917). Cambridge University Press, Cambridge.
Tuttle, B. A. *et al.* (1993). Highly oriented, chemically prepared $Pb(Z_r, T_i)O_3$ thin film. *J. Am. Ceram. Soc.* **76,** 1537–1544.
Weaire, D. and Rivier, N (1984). Soap, cells and statistics—random patterns in two dimensions. *Contemp. Phys.* **25,** 593–599.
Yong, Z., Hanson, M. T. and Kovacevic, R. (1994). Topological measure of brittle fragmentation. *Int. J. Solids Struct.* **31,** 391–415.
Yong, Z. (1994a). Non-orthogonal Principal Stresses. Submitted.
Yong, Z. (1994b). A rational source of plane fractals and application to fragmentation analysis of thin plates. Submitted.
Zimmermann, M. H. and Brown, C. L. (1971). *Trees—Structure and Function*. Springer, New York.